SIAM J. APPL. MATH.
Vol. 32, No. 4, June 1977

NONLINEAR DYNAMIC THEORY FOR A DOUBLE-DIFFUSIVE CONVECTION MODEL*

L. A. RUBENFELD AND W. L. SIEGMANN†

Abstract. The dynamical behavior of small-norm solutions to a simple fluid-loop model describing convection in a two-constituent fluid is discussed. Asymptotic techniques are developed to describe the dynamic behavior of solutions near those parts of the linear stability boundary where one eigenvalue passes through zero (exchange of stabilities), where two eigenvalues become purely imaginary conjugates (Hopf bifurcation), and where two eigenvalues coalesce to zero.

1. Introduction. Double-diffusive convection denotes convective motion in a fluid which possesses two density-altering constituents with differing molecular diffusivities, such as certain motions in the oceans and some lakes where the two properties are salt and heat. Of particular interest is the situation when, in the absence of motion, constituent gradients are present which produce density gradients of opposite signs. An excellent account of known properties of double-diffusive convection in a Newtonian fluid is contained in a recent monograph [1].

In [2] a simple fluid loop model exhibiting double-diffusive convection was derived and studied. In this model fluid was confined within a vertical circular loop of very small cross-section and could flow only in the circumferential direction of the loop. The loop was imbedded in a motionless medium with which it could exchange "heat" and "salt" at different rates, proportional to the instantaneous difference of the heat and salt values in the medium and loop. Assuming an incompressible Boussinesq fluid, and a viscous force proportional to the velocity, a system of equations was derived in [2] for the time behavior of the fluid velocity and the Fourier sine and cosine components of the salt concentration and temperature. This system of five ordinary differential equations possesses a "conductive" solution, i.e., one with no fluid motion and the same (linear) vertical stratification of salt concentration and temperature in the loop as in the medium. The deviations from this conductive state satisfy another system of five nonlinear, coupled, ordinary differential equations, involving four dimensionless quantities. They are a Prandtl number (σ), two Rayleigh numbers (R and R_s, associated with temperature and salt concentration respectively), and a Schmidt number (μ). The Schmidt number was assumed to lie in the range $0<\mu<1$, reflecting the assumption that the exchange of salt occurs at a slower rate than that of heat.

The aim of [2] was to investigate the region of the R-R_s plane, for fixed σ and μ, in which the conductive state is globally stable. Using energy integral techniques (see [3]), the largest such region was found and, moreover, it was proved that all perturbations of the conductive solution in this region decayed to zero with time.

The purpose of the present work is to investigate the evolution of the flow near the linear stability boundaries. The problem is made interesting because two

* Received by the editors July 31, 1975, and in final revised form September 10, 1976.

† Department of Mathematical Sciences, Rensselaer Polytechnic Institute, Troy, New York 12181. The work of the second author was supported in part by the Army Research Office, Durham, under Contract DAH004-73-C-0028.

parameters (R and R_s) are required to define the linear stability boundaries, indicated in Fig. 1 by the solid parts of the two lines $L^{(1)}$ and $L^{(2)}$. The notation in this figure is explained in the next section, where the equations are formulated and the linear stability results of [2] are summarized. The behavior of the eigenvalues of the coefficient matrix of the linearized problem is also discussed near the stability boundaries, as a prelude to the development of amplitude equations governing small but finite-amplitude disturbances.

Steady "convective" solutions, i.e., motions independent of time with non-zero fluid velocity, are the simplest states into which the conductive solution could bifurcate. Starting from results in [2], we discuss this type of solution in § 3 for parameter values near the linear stability boundaries. Diagrams (Figs. 2–4) of the standard type are used to display the variety of possible bifurcations.

On line $L^{(1)}$ of Fig. 1, there is a simple zero eigenvalue of the matrix of coefficients in the linearized problem which gives rise to the simplest bifurcation phenomena [4], [5], [6]. In § 4 we use a derivative expansion procedure (discussed in [17]) to derive the amplitude equation governing the motion. It is also shown there how this equation must be modified in a neighborhood of the point $P^{(1)}$. Similarly, in § 5, appropriate amplitude equations are derived for the bifurcated states in a neighborhood of the line $L^{(2)}$ of Fig. 1. On this line, two eigenvalues of the linear matrix become purely imaginary conjugates, leading to so-called Hopf bifurcation [8]. We show that near $L^{(2)}$, and to the left of the point $P^{(3)}$ of Fig. 1, a stable small-norm periodic solution bifurcates, but that this cannot take place to the right of $P^{(3)}$.

In § 6, the dynamics near $P^{(0)}$ of Fig. 1 is discussed. At this point, two eigenvalues of the matrix of coefficients of the linearized system coalesce to zero, and modifications of the method used near the line $L^{(1)}$ must be incorporated. The qualitative behavior of solutions to the amplitude equation are discussed.

We remark that this model permits a simple analytic analysis of the various bifurcation phenomena which can be anticipated for the Navier–Stokes equations, without encountering the computational difficulties of that more realistic fluid model. The results of § 5 concerning the point $P^{(3)}$ were unexpected and not predicted by Sani [9], who considered the analogous problem for the Navier–Stokes equations. Moreover, Sani's calculations, using the Stuart–Watson method, break down completely near the point $P^{(0)}$, since his results predicted singularities in the coefficients of the amplitude equation there. The incorrect description of the bifurcation near $P^{(0)}$ can be traced directly to the inability of the classical procedure to handle the double zero eigenvalue. The resolution of this difficulty for the Navier–Stokes equations follows in a manner analogous to that for our loop model, as will be reported elsewhere.

2. Formulation and results of linear theory. It is convenient to define two new dimensionless parameters δ and ν, in terms of the Rayleigh numbers R and R_s used in [2]:

$$\nu=\sigma R-\frac{(\sigma+\mu)}{(1-\mu)},\qquad \delta=\sigma R_s-\frac{\mu^2(\sigma+1)}{(1-\mu)}. \tag{2.1}$$

This translation moves the point $P^{(0)}$ in the R-R_s plane in Fig. 2 of [2], to the origin in the ν-δ plane.

In terms of the four dimensionless parameters σ, μ, ν and δ, equations (3.4) in [2] become the matrix system

(2.2) $$\dot{\mathbf{x}} = A\mathbf{x} + x_4 N\mathbf{x}, \qquad \mathbf{x}(0) \text{ given},$$

where $\cdot$ denotes d/dt, $\mathbf{x}$ is a 5×1 column vector with components $x_1, \cdots, x_5$, and the matrices A (of coefficients of the linearized system) and N are

(2.3) $$A = \begin{bmatrix} -1 & 0 & 0 & 0 & 0 \\ 0 & -\mu & 0 & 0 & 0 \\ 0 & 0 & -1 & 1 & 0 \\ 0 & 0 & \nu + \dfrac{\sigma+\mu}{1-\mu} & -\sigma & -\delta - \dfrac{\mu^2(\sigma+1)}{(1-\mu)} \\ 0 & 0 & 0 & 1 & -\mu \end{bmatrix},$$
$$N = \begin{bmatrix} 0 & 0 & -1 & 0 & 0 \\ 0 & 0 & 0 & 0 & -1 \\ 1 & 0 & 0 & 0 & 0 \\ 0 & 0 & 0 & 0 & 0 \\ 0 & 1 & 0 & 0 & 0 \end{bmatrix},$$

with

(2.4) $$0 < \sigma, \qquad 0 < \mu < 1.$$

The conductive solution is $\mathbf{x} = 0$.

Certain principal features of the behavior of solutions to (2.2) and (2.3) are depicted in Fig. 1. The solid parts of the lines $L^{(1)}$ and $L^{(2)}$ separate regions of linear stability and instability in the ν-δ plane. The eigenvalues λ of A satisfy

(2.5) $$(\lambda+1)(\lambda+\mu)[\lambda^3 + \Delta\lambda^2 + (\delta-\mu)\lambda + (\delta-\mu\nu)] = 0,$$

where

(2.6) $$\Delta \equiv \sigma + \mu + 1 > 0.$$

These can be shown to possess the following properties:

To the left of both $L^{(1)}$ and $L^{(2)}$: All eigenvalues of A have negative real parts. This is the region of linear stability, where all solutions of the linearized system $\dot{\mathbf{x}} = A\mathbf{x}$ decay to zero. It is possible, however, that solutions to (2.2) may not decay to zero.

To the right of either $L^{(1)}$ or $L^{(2)}$: Some of the eigenvalues of A have positive real parts, and some solutions of the linearized system grow exponentially in time.

On and near the solid part of $L^{(1)}$: On the solid part of $L^{(1)}$ ($\delta = \mu\nu$, $\nu < 0$), four eigenvalues have negative real parts and one is zero (except at $P^{(0)}$). The zero eigenvalue corresponds to neutral stability, and by continuity, the four with negative real parts will retain this characteristic slightly away from $L^{(1)}$. By investigating how the zero root of (2.5) behaves for $\delta - \mu\nu \ll 1$, and $\nu < 0$, we

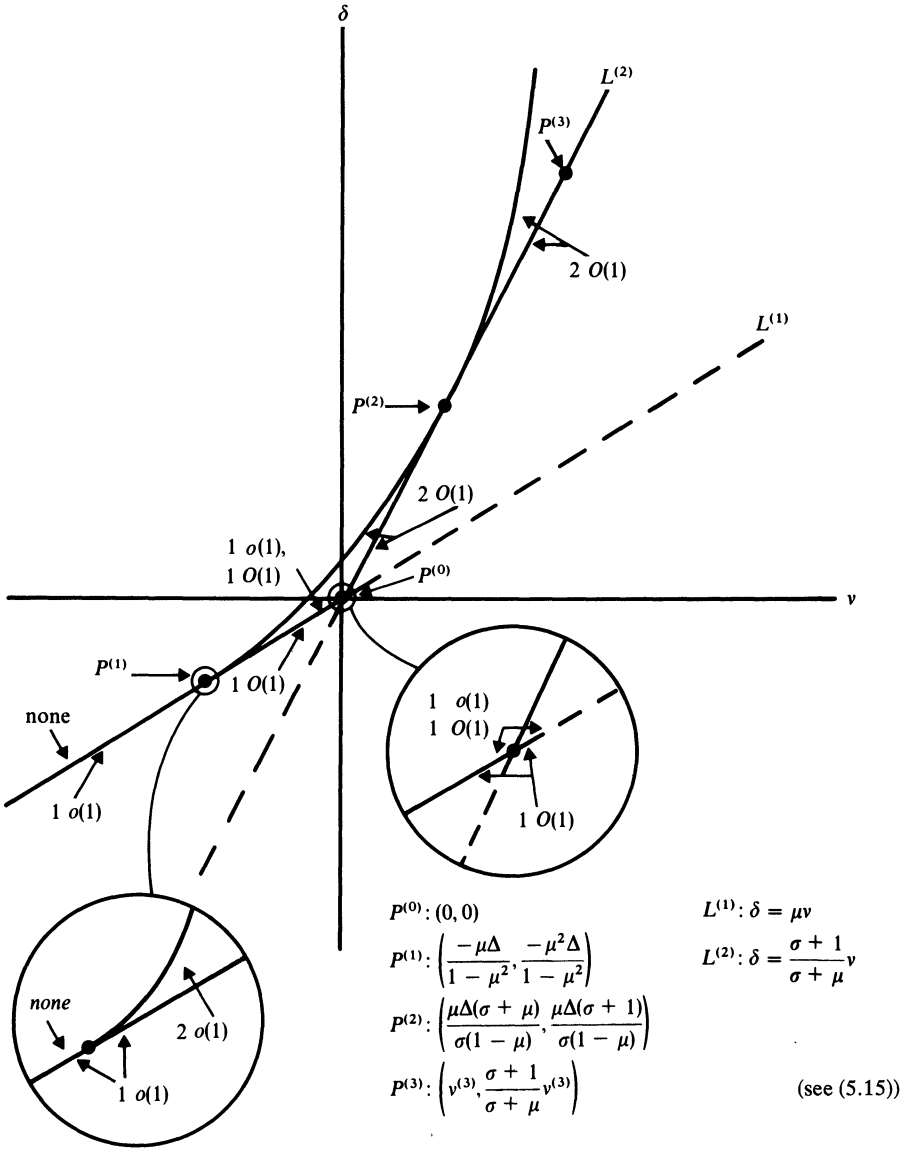

FIG. 1

easily derive that the small root $\lambda^{(1)}$ is

$$\text{(2.7)}\quad \lambda^{(1)} = \frac{(\delta-\mu\nu)}{\nu(1-\mu)} + \frac{(\delta-\mu\nu)^2[\nu(1-\mu)+\Delta]}{\nu^3(1-\mu)^3} + O((\delta-\mu\nu)^3), \qquad \delta-\mu\nu \ll 1.$$

We note that (2.7) is not valid where $\nu \ll 1$, which corresponds to the point $P^{(0)}$ discussed below. We also note that $\lambda^{(1)}$ is negative above the solid part of $L^{(1)}$ (since $\nu < 0$ and $\delta - \mu\nu > 0$) and positive below. Thus there is exponential decay above, and growth below, the solid portion of $L^{(1)}$.

On and near the solid portion of $L^{(2)}$: On the solid portion of the line $L^{(2)}$ $(\delta=((\sigma+1)/(\sigma+\mu))\nu,\ \nu>0)$, the roots of (2.5) are given by

$$\lambda=-1,\ -\mu,\ -\Delta,\ \pm i\left[\frac{(1-\mu)\nu}{\sigma+\mu}\right]^{1/2}. \tag{2.8}$$

Near this part of $L^{(2)}$ the three negative roots retain negative real parts, and the behavior of the imaginary roots $\lambda_{\pm}^{(2)}$ near $L^{(2)}$ is

$$\lambda_{\pm}^{(2)}=\pm i\left[\frac{(1-\mu)\nu}{\sigma+\mu}\right]^{1/2}+\frac{\left(\delta-\frac{(\sigma+1)}{(\sigma+\mu)}\nu\right)}{\left(\Delta^2+\frac{\nu(1-\mu)}{(\sigma+\mu)}\right)}\left[\frac{-(\Delta-1)}{2}\pm\frac{i\left(\Delta+\frac{\nu(1-\mu)}{\sigma+\mu}\right)}{2\left(\frac{\nu(1-\mu)}{\sigma+\mu}\right)^{1/2}}\right]+\cdots, \tag{2.9}$$

$$\delta-\left(\frac{\sigma+1}{\sigma+\mu}\right)\nu\ll 1.$$

On $L^{(2)}$ periodic solutions of the linear system exist. As before, (2.9) is invalid near $\nu=0$.

At and near $P^{(0)}$: At $P^{(0)}$ $(\delta=\nu=0)$, (2.5) has three negative and two zero roots. The solution to the linear system may thus exhibit linear growth in time. To determine the behavior of the zero roots near $P^{(0)}$, we note that the small roots are not analytic functions of δ and ν there. It can be shown that the two small roots λ_0 of (2.5) satisfy the quadratic equation

$$\lambda_0^2+a\lambda_0+b=0,\qquad \delta,\ \nu\ll 1 \tag{2.10}$$

where

$$\begin{aligned} a&=\frac{(\delta-\nu)}{\Delta}-\frac{(\delta-\mu\nu)}{\Delta^2}+\frac{(\delta-\nu)^2}{\Delta^3}-\frac{3(\delta-\nu)(\delta-\mu\nu)}{\Delta^4}+\frac{2(\delta-\mu\nu)^2}{\Delta^5}+\cdots,\\ b&=\frac{(\delta-\mu\nu)}{\Delta}+\frac{(\delta-\nu)(\delta-\mu\nu)}{\Delta^3}-\frac{(\delta-\mu\nu)^2}{\Delta^4}+\cdots. \end{aligned} \tag{2.11}$$

Equation (2.10) will lead (see § 6) to a second-order amplitude equation describing the time evolution of the zero solution of (2.2) near $P^{(0)}$.

3. The approximate steady states and bifurcation diagrams. It was shown in [2] that the nontrivial steady state solutions of (2.2) are given by

$$\mathbf{x}_{\text{steady}}^T=\left(\frac{-P}{1+P},\frac{-P}{\mu^2+P},\frac{\pm P^{1/2}}{1+P},\ \pm P^{1/2},\ \frac{\pm\mu P^{1/2}}{\mu^2+P}\right), \tag{3.1}$$

where "T" denotes transpose and the *positive* quantity P is

$$(2\sigma/\mu)P=(\nu/\mu-\delta+\Delta)\pm[(\nu/\mu-\delta+\Delta)^2-(4\sigma/\mu)(\delta-\mu\nu)]^{1/2}. \tag{3.2}$$

The steady states (3.1) exist in those regions of the ν-δ plane where the right hand side of (3.2) is real and positive. In the ν-δ plane of Fig. 1, these regions are:

No convective steady states. On that part of $L^{(1)}$ lying to the left of $P^{(1)}$; also to the left of the parabolic curve and above $L^{(1)}$. (We proved [2] that this region of linear stability containing no nontrivial steady states was a region of global stability, wherein all solutions of (2.2) decay to zero.)

One pair of convective steady states. Below $L^{(1)}$; on that part of $L^{(1)}$ lying to the right of $P^{(1)}$; and on the whole parabolic curve.

Two pairs of convective steady states. In the region between the parabolic curve and the line $L^{(1)}$. Note the three-sided region in Fig. 1 with vertices $P^{(0)}$, $P^{(1)}$, and $P^{(2)}$, and the region above $P^{(2)}$ between the parabola and $L^{(2)}$, where additional steady states exist in the linear stability regime; these are regions of subcritical instability, where linear theory predicts decay but finite-amplitude disturbances may grow.

Approximate expressions for the steady states near linear stability boundaries are important for understanding the time behavior of perturbations of the zero solution of (2.2). These expressions have the following form:

Near the solid part of $L^{(1)}$: We obtain from (3.2)

$$\begin{aligned}\left(\frac{2\sigma}{\mu}\right)P=&\frac{\nu(1-\mu^2)+\mu\Delta}{\mu}-(\delta-\mu\nu)\\ &\pm\left[\frac{(\nu(1-\mu^2)+\mu\Delta)^2}{\mu^2}-2(\delta-\mu\nu)\left(\frac{2\sigma}{\mu}+\frac{\nu(1-\mu^2)+\mu\Delta}{\mu}\right)\right.\\ &\left.+(\delta-\mu\nu)^2\right]^{1/2}.\end{aligned} \tag{3.3}$$

The condition $P>0$ requires the following numbers and sizes of allowable steady states (each root P yields a pair of steady states):

$\nu+\frac{\mu\Delta}{1-\mu^2}$ "large" (compared to $\delta-\mu\nu$):

$\nu>\frac{-\mu\Delta}{1-\mu^2}$ $\begin{cases}\text{(i) one large (upper sign) and one small } O(\delta-\mu\nu) \text{ root (lower sign) if } \delta+\mu\nu>0,\\ \text{(ii) one large root (upper sign) if } \delta-\mu\nu<0;\end{cases}$

$\nu<\frac{-\mu\Delta}{1-\mu^2}$ $\begin{cases}\text{(i) no roots if } \delta-\mu\nu>0,\\ \text{(ii) one small } O(\delta-\mu\nu) \text{ root (lower sign) if } \delta-\mu\nu<0.\end{cases}$

$\nu+\frac{\mu\Delta}{1-\mu^2}$ "small' (compared to $\delta-\mu\nu$):

All positive roots, where they exist in the neighborhood of $P^{(1)}$, are small. Thus, near $P^{(1)}$ where the boundary between steady states and no steady states is tangent to the linear stability boundary $L^{(1)}$, the possibility arises of multiple pairs of small-norm steady states. The exact orders of magnitude of the roots depend on the relative orders of magnitude of $\delta-\mu\nu$ and $\nu+\mu\Delta\cdot(1-\mu^2)^{-1}$.

Near the solid part of $L^{(2)}$: From (3.2) we derive

$$\left(\frac{2\sigma}{\mu}\right)P=\left[\frac{\sigma(1-\mu)\nu}{\mu(\sigma+\mu)}+\Delta\right]\pm\left[\left(\frac{\sigma(1-\mu)\nu}{\mu(\sigma+\mu)}-\Delta\right)^2+O\left(\delta-\left(\frac{\sigma+1}{\sigma+\mu}\right)\nu\right)\right]^{1/2} \tag{3.4}$$

Clearly, from (3.4), there are never any roots which are small with $\delta - ((\sigma+1)/(\sigma+\mu))\nu$. Note that the point of tangency $P^{(2)}$ in Fig. 1 is the only point on $L^{(2)}$ where the square root in (4.5) vanishes. Thus $P^{(2)}$ is the only point on $L^{(2)}$ where just one pair of steady states exists.

Near $P^{(0)}$: We see from (3.2), for ν and δ small, there is always one large root (upper sign) and, where a second root (lower sign) exists between the parabolic curve and $L^{(1)}$, it is small.

In Fig. 1 we have indicated the number and size of the steady states in regions near the linear stability boundaries $L^{(1)}$ and $L^{(2)}$. Using standard notation, "small" is denoted by $o(1)$ and "large" by $O(1)$. The number indicates how many pairs of nonzero steady states exist.

In Figs. 2–4 we show plots of bifurcation diagrams [4] of "norm of solution", $\|\mathbf{x}\|$, versus bifurcation parameter. We chose as a measure of norm the positive quantity P given by (3.2) which, by (3.1) and [2], is the square of the steady fluid velocity. If we fix δ, then ν serves as a bifurcation parameter, and Figs. 2–4 show P vs. ν for different ranges of δ.

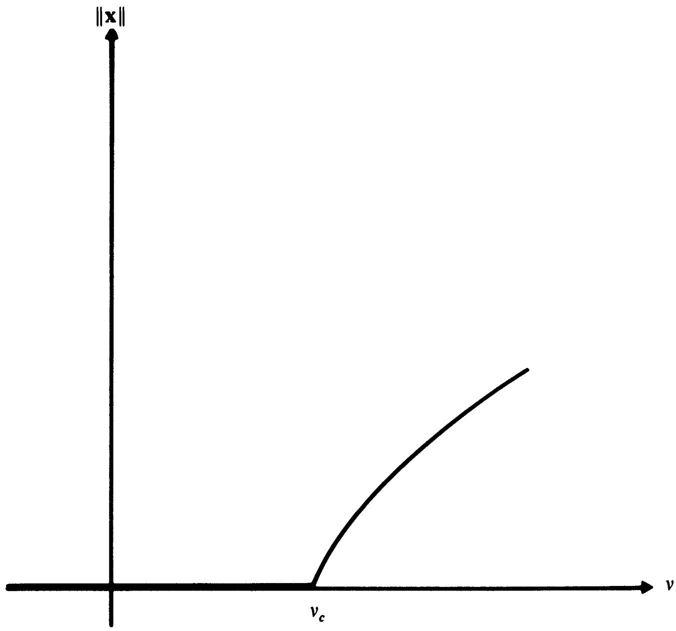

$$\delta \leqq \delta^{(1)} = \frac{-\mu^2\Delta}{(1-\mu^2)}$$

$$\nu_c = \frac{\delta}{\mu}$$

FIG. 2

From each point of the solid portion of $L^{(1)}$, a small-norm steady state bifurcates in the usual manner [4]. Figure 2 reflects the fact that if δ is equal to or below its value $\delta^{(1)}$ at $P^{(1)}$, there will be no nonzero steady states as ν increases

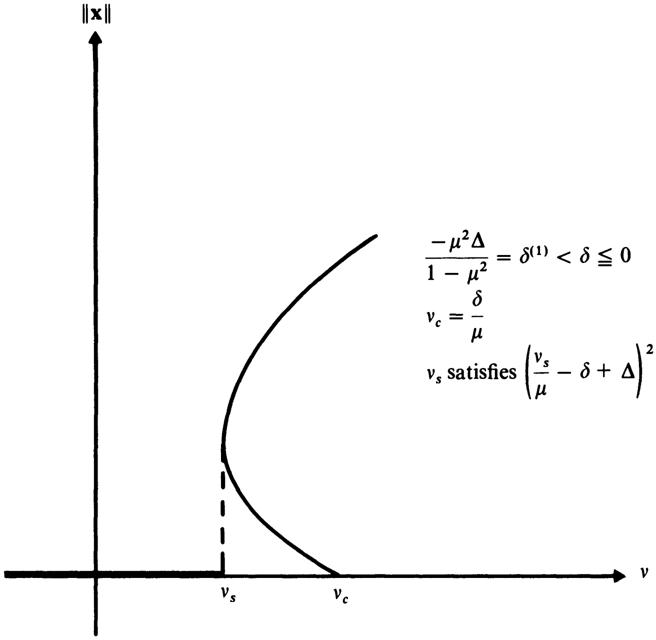

$$\frac{-\mu^2\Delta}{1-\mu^2} = \delta^{(1)} < \delta \leqq 0$$

$$v_c = \frac{\delta}{\mu}$$

$$v_s \text{ satisfies } \left(\frac{v_s}{\mu} - \delta + \Delta\right)^2 - \frac{4\sigma}{\mu}(\delta - \mu v_s) = 0$$

FIG. 3

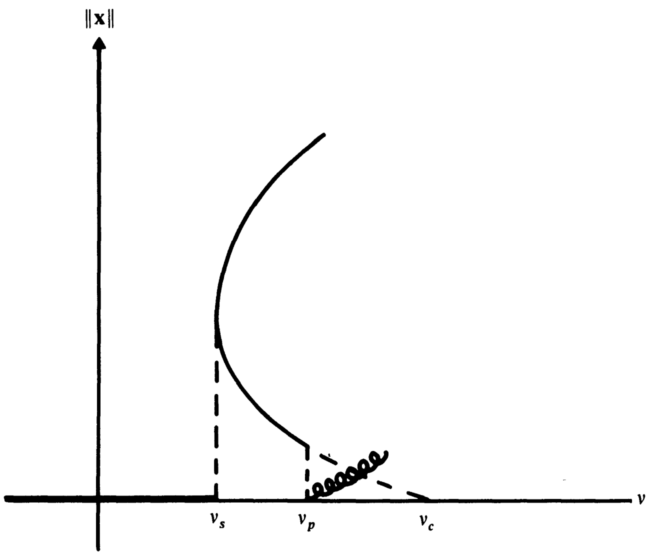

$$\delta > 0$$

$$v_c = \frac{\delta}{\mu}$$

$$v_s \text{ satisfies } \left(\frac{v_s}{\mu} - \delta + \Delta\right)^2 - \frac{4\sigma}{\mu}(\delta - \mu v_s) = 0$$

$$v_p = \frac{\sigma + \mu}{\sigma + 1} - \delta$$

FIG. 4

from $-\infty$, until the line $L^{(1)}$ is reached, where ν attains the critical value $\nu_c = \delta\mu^{-1}$. One solution then bifurcates from the zero solution at $\nu = \nu_c$, its norm remaining small for ν in a neighborhood of ν_c.

In Fig. 3, δ is above its value at $P^{(1)}$ and negative. As ν increases from $-\infty$, there are no nonzero steady states until the value $\nu = \nu_s$, corresponding to the parabolic curve, is reached, at which point there is exactly one steady state. For larger ν, there will be two pairs of steady states, though not necessarily of small norm. As ν increases further, the value $\nu = \nu_c$ is again reached, and a small-norm bifurcation occurs from the zero solution in a subcritical manner. This solution is expected to be unstable. As ν increases beyond ν_c, only a large-norm steady solution remains. Near the point $P^{(1)}$ in figure 1, ν_s and ν_c are nearly equal. Thus, there are two small-norm solutions in this case for $\nu_s < \nu < \nu_c$, as can be seen from Fig. 3 with $\delta \approx \delta^{(1)}$. In § 4, we will show that the equations governing the approximate solutions near $P^{(1)}$ change from having cubic to quintic nonlinearities.

The plot in Fig. 4 is for the case $\delta > 0$. Here, the situation as ν increases from $-\infty$ to ν_s is as above. However, the point ν_p is reached before ν_c. This corresponds to the line $L^{(2)}$ (see Fig. 1 with $\delta > 0$). Since two imaginary eigenvalues of the linear matrix A of (2.3) exist on $L^{(2)}$, we expect a periodic solution to bifurcate from ν_p. This is indicated by the wiggly line of Fig. 4. In fact, it is shown in § 6 that such a small-norm, periodic bifurcation may not occur at all points on $L^{(2)}$. We also note that ν_p and ν_c are nearly equal near the point $P^{(0)}$ in Fig. 1. This proximity gives rise to differing behavior near $P^{(0)}$ due to the fact that every neighborhood of $P^{(0)}$ contains points on both $L^{(1)}$ and $L^{(2)}$.

We now explain why the parabolic steady-state boundary in the ν-δ plane of Fig. 1 must in fact be tangent to the linear stability boundary $L^{(1)}$. Let $(\nu^{(1)}, \delta^{(1)})$ be the point of tangency $P^{(1)}$ of Fig. 1, and suppose that the parabola and $L^{(1)}$ were not tangent at $P^{(1)}$. Then, starting from $P^{(1)}$, it would be possible to enter the region between $L^{(1)}$ and the parabola along certain straight lines in the ν-δ plane. Let the equation of one such line be given by

$$a(\nu - \nu^{(1)}) + b(\delta - \delta^{(1)}) = 0. \tag{3.5}$$

Define the variable τ by

$$\tau = c(\nu - \nu^{(1)}) + d(\delta - \delta^{(1)}), \qquad ad - bc \neq 0. \tag{3.6}$$

From (3.5) and (3.6) we can solve for ν and δ in terms of τ, with $\tau = 0$ corresponding to the point $(\nu^{(1)}, \delta^{(1)})$. In terms of τ, the steady-state equations $A\mathbf{x} + x_4 N\mathbf{x} = 0$ from (2.2) can be written in the form

$$(L_0 + \tau L_1)\mathbf{x} + x_4 N\mathbf{x} = 0, \tag{3.7}$$

where L_0 and L_1 are matrices determined from (2.2), (2.3), (3.5), and (3.6). It is easy to verify that

(i) L_0 has a simple zero eigenvalue,

(ii) $L_0 + \tau L_1$ has a simple real eigenvalue $\mu(\tau)$ such that $\mu(0) = 0$, $\mu'(0) \neq 0$.

By [10, Thm. (3.1), p. 269], there exists a one-parameter family $\mathbf{x} = \mathbf{x}(\varepsilon)$, $\tau = \tau(\varepsilon)$ of solutions to (3.7) such that $\mathbf{x}(0) = 0$, $\tau(0) = 0$. That is, in any small one-dimensional neighborhood of $P^{(1)}$, i.e., one restricted by (3.5), there cannot be two independent small-norm steady states bifurcating from the zero solution.

However, earlier arguments in this section show that two steady states bifurcate from $P^{(1)}$. Thus, the parabola and $L^{(1)}$ must necessarily be tangent at $P^{(1)}$, thereby avoiding contradiction of the theorem. It is interesting that there are indeed two solutions bifurcating from $P^{(1)}$, but this does not contradict classical bifurcation theory. This phenomenon is due to the occurrence of two small parameters describing proximity to the point $P^{(1)}$, not just one (such as τ, above) which restricts the approach to $P^{(1)}$. In such a situation, the theory evidently differs from the single parameter case and is currently under investigation.

4. Dynamic behavior near $L^{(1)}$. We will now consider the time-dependent behavior of initially small solutions of (2.2) and (2.3) near the linear stability boundary $\delta = \mu\nu$, $\nu < 0$. We assume that the initial condition $\mathbf{x}(0)$ in (2.2) is of the form

$$\mathbf{x}(0) = \varepsilon \mathbf{x}_0, \qquad 0 < \varepsilon \ll 1, \tag{4.1}$$

where ε is some measure of the size of the initial vector $\mathbf{x}(0)$. If we define

$$\mathbf{u}(t) = \varepsilon^{-1}\mathbf{x}(t), \qquad \theta = \delta - \mu\nu \ll 1, \tag{4.2}$$

then (2.2) and (2.3) become

$$\dot{\mathbf{u}} = A_1\mathbf{u} + \theta B_1\mathbf{u} + \varepsilon u_4 N\mathbf{u}, \qquad \mathbf{u}(0) = \mathbf{x}_0,$$

$$A_1 = \begin{bmatrix} -1 & 0 & 0 & 0 & 0 \\ 0 & -\mu & 0 & 0 & 0 \\ 0 & 0 & -1 & 1 & 0 \\ 0 & 0 & \nu + \dfrac{(\sigma+\mu)}{(1-\mu)} & -\sigma & -\mu\nu - \dfrac{\mu^2(\sigma+1)}{(1-\mu)} \\ 0 & 0 & 0 & 1 & -\mu \end{bmatrix}, \tag{4.3}$$

$$B_1 = \begin{bmatrix} 0 & 0 & 0 & 0 & 0 \\ 0 & 0 & 0 & 0 & 0 \\ 0 & 0 & 0 & 0 & 0 \\ 0 & 0 & 0 & 0 & -1 \\ 0 & 0 & 0 & 0 & 0 \end{bmatrix},$$

and the matrix N is given by (2.3). Note that A_1 is the matrix A of (2.3) with $\delta = \mu\nu$. We seek an asymptotic solution of (4.3) for ε, $\theta \ll 1$.

The solution of the linear system

$$\dot{\mathbf{u}} = A_1\mathbf{u} \tag{4.4}$$

is given by

$$\mathbf{u} = \alpha(0, 0, \mu, \mu, 1)^T + (\text{decay}). \tag{4.5}$$

The first term on the right of (4.5) is an arbitrary multiple, α, of the vector $(0, 0, \mu, \mu, 1)^T$, which is the eigenvector of A_1 corresponding to the zero eigenvalue of the linearized system on $L^{(1)}$. The other terms on the right of (4.5) are decaying terms which correspond to the remaining eigenvalues of A_1, with negative real parts on $L^{(1)}$. In our subsequent analysis, we will ignore these terms.

To investigate deviations of (4.5) caused by the small terms in (4.3), the constant multiple α is assumed to be a slowly-varying function of time. Since boundedness must be invoked, the following result is useful: If $\boldsymbol{\beta} = (\beta_1, \cdots, \beta_5)^T$ is a constant vector, then the most general solution, bounded as $t \to \infty$, of the inhomogeneous linear equation

$$\dot{\mathbf{v}} - A_1\mathbf{v} = \boldsymbol{\beta} + (\text{decay}) \tag{4.6}$$

is given by

$$\mathbf{v} = \alpha(0, 0, \mu, \mu, 1)^T + (\text{decay}) + (\beta_1, \mu^{-1}\beta_2, \beta_3 - \beta_5, -\beta_5, 0)^T, \tag{4.7}$$

providing that

$$\beta_4 + \left(\nu + \frac{\sigma+\mu}{1-\mu}\right)\beta_3 - \left(\nu + \mu\frac{\sigma+1}{1-\mu}\right)\beta_5 = 0. \tag{4.8}$$

The condition (4.8) prevents the appearance in (4.7) of a term linear in t.

We will use an asymptotic procedure similar to that in [7], [13], and [14], related to that in [18], and used successfully in [15].[1] We represent the solution of (5.3) in the form

$$\mathbf{u} \sim \alpha(t)(0, 0, \mu, \mu, 1)^T + (\text{decay}) + \sum_{\substack{i,j=0\\ i+j>0}}^{\infty} \varepsilon^i\theta^j\mathbf{u}^{(ij)}(t; \alpha), \tag{4.9}$$

where

$$\dot{\alpha} = \sum_{\substack{i,j=0\\ i+j>0}}^{\infty} \varepsilon^i\theta^j\alpha^{(ij)}. \tag{4.10}$$

From (4.9) we find

$$\dot{\mathbf{u}} \sim \dot{\alpha}(t)(0, 0, \mu, \mu, 1)^T + (\text{decay}) + \sum_{\substack{i,j=0\\ i+j>0}}^{\infty} \varepsilon^i\theta^j[\mathbf{u}_t^{(ij)} + \dot{\alpha}\mathbf{u}_\alpha^{(ij)}], \tag{4.11}$$

where $\mathbf{u}_t^{(ij)}$ and $\mathbf{u}_\alpha^{(ij)}$ are partial derivatives of the vector $\mathbf{u}^{(ij)}$ with respect to t and α, respectively. Using (4.10) and (4.11) in (4.3), and equating coefficients of $\varepsilon^i\theta^j$, we find the $\mathbf{u}^{(ij)}$ satisfy the following recursive system of equations:

$$L\mathbf{u}^{(10)} \equiv \mathbf{u}_t^{(10)} - A_1\mathbf{u}^{(10)} = -\alpha^{(10)}(0, 0, \mu, \mu, 1)^T - \mu\alpha^2(\mu, 1, 0, 0, 0)^T, \tag{4.12}$$

$$L\mathbf{u}^{(01)} = -\alpha^{(01)}(0, 0, \mu, \mu, 1)^T - \alpha(0, 0, 0, 1, 0)^T, \tag{4.13}$$

$$\begin{aligned} L\mathbf{u}^{(20)} = &-\alpha^{(20)}(0, 0, \mu, \mu, 1)^T - \alpha^{(10)}\mathbf{u}_\alpha^{(10)} + \mu\alpha N\mathbf{u}^{(10)} \\ &- \alpha u_4^{(10)}(\mu, 1, 0, 0, 0)^T, \end{aligned} \tag{4.14}$$

[1] See [11], [12] for an alternate procedure using multiscaling.

$$\text{(4.15)}\quad \begin{aligned} L\mathbf{u}^{(11)} &= -\alpha^{(11)}(0, 0, \mu, \mu, 1)^T - \alpha^{(01)}\mathbf{u}_\alpha^{(10)} - \alpha^{(10)}\mathbf{u}_\alpha^{(01)} \\ &\quad + B_1\mathbf{u}^{(10)} + \mu\alpha N\mathbf{u}^{(01)} - \alpha u_4^{(01)}(\mu, 1, 0, 0, 0)^T, \end{aligned}$$

$$\text{(4.16)}\quad L\mathbf{u}^{(02)} = -\alpha^{(02)}(0, 0, \mu, \mu, 1)^T - \alpha^{(01)}\mathbf{u}_\alpha^{(01)} + B_1\mathbf{u}^{(01)}.$$

Note that the operator L is defined in (4.12).

Each of equations (4.12)–(4.16) is of the type (4.6). Therefore, applying (4.7) and (4.8), we can derive from each of (4.12)–(4.16) a boundedness condition, from which we can determine the $\alpha^{(ij)}$ in (4.10), and a solution consisting of a bounded particular solution plus an arbitrary multiple of the solution to the homogeneous equation $L\mathbf{v} = 0$. We explicitly neglect the homogeneous solutions in each of (4.12)–(4.16). Thus the homogeneous solution is represented solely in the first term on the right side of (4.9). This arbitrary choice is related to that used in certain applications of the method of averaging [7].

Proceeding in this manner, we can compute $\alpha^{(10)}$, $\alpha^{(01)}$, $\mathbf{u}^{(10)}$, and $\mathbf{u}^{(01)}$ from (4.12) and (4.13). Then we compute $\alpha^{(20)}$, $\alpha^{(11)}$, and $\alpha^{(02)}$ from (4.14)–(4.16), noting that $\mathbf{u}^{(20)}$, $\mathbf{u}^{(11)}$, and $\mathbf{u}^{(02)}$ are not needed for this purpose. Substituting into (4.9) and (4.10), using (4.2), and defining

$$\text{(4.17)}\quad R = \varepsilon\alpha,$$

we find the formal asymptotic description for the solution $\mathbf{x}(t)$ of (2.2) is given by

$$\text{(4.18)}\quad \begin{aligned} \mathbf{x}(t) &\sim R(t)(0, 0, \mu, \mu, 1)^T + (\text{decay}) - R^2(t)(\mu^2, 1, 0, 0, 0)^T \\ &\quad + \nu^{-1}(1-\mu)^{-1}(\delta - \mu\nu)R(t)(0, 0, 1-\mu, 1, 0)^T + \cdots, \end{aligned}$$

where $R(t)$ satisfies

$$\text{(4.19)}\quad \begin{aligned} \frac{dR}{dt} &= R\left[\frac{(\delta-\mu\nu)}{\nu(1-\mu)} + \frac{(\nu(1-\mu)+\Delta)(\delta-\mu\nu)^2}{\nu^3(1-\mu)^3}\right] \\ &\quad - \frac{\mu}{\nu(1-\mu)}[\nu(1-\mu^2)+\mu\Delta]R^3, \qquad \delta - \mu\nu \ll 1, \\ R(0) &= O(\varepsilon). \end{aligned}$$

Note that the coefficient of R in (4.19) is the first two terms in powers of $\delta - \mu\nu$, of the linear growth rate near the stability boundary $L^{(1)}$ (see (2.7)).

From (4.19) and its solution we can deduce the following results:

$\nu(1-\mu^2) + \mu\Delta < 0$:

(a) $R(t)$ (and thus $\mathbf{x}(t)$) decays to zero for $\delta - \mu\nu > 0$. This is expected since this case is in the globally stable region above $L^{(1)}$ and to the left of the parabolic arc.

(b) $R(t)$ grows to an $O(|\delta - \mu\nu|^{1/2})$ steady state when $\delta - \mu\nu < 0$. This is the unique $o(1)$ steady state indicated in Fig. 1.

$\nu(1-\mu^2) + \mu\Delta > 0$, $\nu < 0$:

(a) If $\delta - \mu\nu > 0$, then, depending upon the size of the initial condition, R may decay to zero or become large. This is a typical result in a subcritical region. The fact that R gets large merely means that no nontrivial $o(1)$ solution exists in this region, as is indicated also in Fig. 1.

(b) If $\delta-\mu\nu<0$, then all solutions to (4.19) get large. This again indicates no nontrivial small steady state. In fact, the solutions would be expected to grow until they reach the $O(1)$ solution indicated in Fig. 1.

We note that (4.19) is not valid near $P^{(0)}$ where $\nu\to 0$. In addition, it breaks down near the point $P^{(1)}$ on $L^{(1)}$ where $\nu(1-\mu^2)+\mu\Delta=0$, since the coefficient of R^3 in (4.19) is small also. We overcome this difficulty by calculating additional terms in the expansions (4.9) and (4.10). Merely listing the outcome of the calculations, we find that the solution of (2.2) is given asymptotically by

$$\mathbf{x}(t)\sim R(t)(0,0,\mu,\mu,1)^T+(\text{decay})+\sum_{j=0}^{3}(\delta-\mu\nu)^j\mathbf{x}_1^{(j)}(R)+\cdots, \tag{4.20}$$

where the vectors $\mathbf{x}_1^{(j)}(R)$ are given in Appendix A. The amplitude $R(t)$ now satisfies

$$\begin{aligned}\frac{dR}{dt}&=R\left[\frac{(\delta-\mu\nu)}{\nu(1-\mu)}+\frac{(\delta-\mu\nu)^2(\nu(1-\mu)+\Delta)}{\nu^3(1-\mu)^3}+K_5(\delta-\mu\nu)^3+K_6(\delta-\mu\nu)^4\right]\\&\quad+R^3\left[-\frac{\mu(\nu(1-\mu^2)+\mu\Delta)}{\nu(1-\mu)}+K_7(\delta-\mu\nu)+O((\delta-\mu\nu)^2)\right]+KR^5,\\R(0)&=O(\varepsilon),\end{aligned} \tag{4.21}$$

where

$$\begin{aligned}K=&\frac{-\mu}{\nu^2(1-\mu)^2}[\mu^3(\nu(1-\mu)+\sigma+\mu)(3\Delta-2\mu\nu)+2\nu((\nu-\sigma)(1-\mu)+\sigma+\mu)]\\&+\frac{3\mu^3}{\nu^3(1-\mu)^3}[\nu(1-\mu^2)+\mu\Delta][\nu(1-\mu)(1+\Delta)+\Delta^2].\end{aligned} \tag{4.22}$$

The quantities K_5, K_6 and K_7 are given in Appendix A, and the quantity indicated as $O((\delta-\mu\nu)^2)$ in (4.21) has been computed in the procedure but is quite long and is not reproduced here.

We observe from (4.21) that new small terms have been added to the R and R^3 coefficients of (4.19) and that an R^5 term appears. The coefficient of R is again the expansion for small $\delta-\mu\nu$ of the linear growth rate near $L^{(1)}$. Away from $P^{(1)}$, where $\nu(1-\mu^2)+\mu\Delta=0$, the coefficient of R^3 in (4.21) is not small, and the R^5 term produces only small corrections to the evolution of the amplitude. However, this term is vital near $P^{(1)}$. At $P^{(1)}$ where $\nu=-\mu\Delta(1-\mu^2)^{-1}$, K has the value $-(1+\mu)\sigma\mu^2\Delta^{-1}$, from (4.22). Therefore, by continuity, K is negative close to $P^{(1)}$. It then follows that in a neighborhood of $P^{(1)}$, specifically between the parabola and the solid portion of $L^{(1)}$ in Fig. 1, there are two small zeros on the right side of (4.21). These correspond to the two additional $o(1)$ steady states indicated in Fig. 1. For small enough initial conditions, the solution of (4.21) in this region will decay to zero, a result of the linear stability of the zero solution. However, for "large enough" initial conditions, R will proceed to one of the two additional steady states mentioned above, the other one being unstable. This is of course typical of the situation in a subcritical regime, as discussed below (4.19).

The difference here is that for $o(1)$ initial conditions, the solution will never grow away from the $o(1)$ regime, as it could for parameters not near $P^{(1)}$.

We note that a value of $R=\tilde{R}$ which causes the right side of (4.21) to vanish must correspond to a steady convective solution. From (4.20), (A.1) and (A.2), the fourth component of the steady solution is

$$\tilde{x}_4^2=\left[\mu^2\tilde{R}^2-\frac{2\mu^3}{\nu(1-\mu)}(\nu(1-\mu)+\Delta)\tilde{R}^4+O(\tilde{R}^6)\right] \tag{4.23}$$
$$+(\delta-\mu\nu)\left[\frac{2\mu}{\nu(1-\mu)}\tilde{R}^2+O(\tilde{R}^4)\right]+O((\delta-\mu\nu)^2).$$

Combining (4.23) with an expression for $\tilde{R}$ (obtained from (4.21)) which is valid away from the neighborhood of $P^{(1)}$, we obtain

$$\tilde{x}_4^2=\frac{\mu(\delta-\mu\nu)}{[\nu(1-\mu^2)+\mu\Delta]}+(\delta-\mu\nu)^2\frac{\mu^2[\nu(1-\mu^2)+(\mu+1)(\sigma+\mu)]}{[\nu(1-\mu^2)+\mu\Delta]^3} \tag{4.24}$$
$$+O((\delta-\mu\nu)^3).$$

Equation (4.24) is precisely the expansion of the exact steady solution, correct to $O((\delta-\mu\nu)^3)$, obtained from (3.1) and (3.3). It is interesting to observe that the expression for the coefficient of the quintic term in (4.21) is necessary to compute the $O((\delta-\mu\nu)^2)$ term in (4.24). Thus, the R^5 term is meaningful even away from the point $P^{(1)}$, in the sense that it provides necessary higher-order corrections to the steady state.

5. Dynamic behavior near $L^{(2)}$. We next consider the behavior in time of solutions of (2.2) and (2.3) satisfying (4.1), near the linear stability boundary $\delta=((\sigma+1)/(\sigma+\mu))\nu$, $\nu>0$. In analogy with the development in § 4, we define

$$\mathbf{u}(t)=\varepsilon^{-1}\mathbf{x}(t), \qquad \eta=\delta-\left(\frac{\sigma+1}{\sigma+\mu}\right)\nu\ll 1, \tag{5.1}$$

where the small parameter η is a measure of distance from the line $L^{(2)}$. The analogues of (4.3) and (4.6)–(4.8) are

$$\dot{\mathbf{u}}=A_2\mathbf{u}+\eta B_1\mathbf{u}+\varepsilon u_4 N\mathbf{u}, \qquad \mathbf{u}(0)=\mathbf{x}_0,$$

$$A_2=\begin{bmatrix}-1 & 0 & 0 & 0 & 0\\ 0 & -\mu & 0 & 0 & 0\\ 0 & 0 & -1 & 1 & 0\\ 0 & 0 & \nu+\dfrac{\sigma+\mu}{1-\mu} & -\sigma & -\left(\dfrac{\sigma+1}{\sigma+\mu}\right)\left(\nu+\dfrac{\mu^2(\sigma+\mu)}{1-\mu}\right)\\ 0 & 0 & 0 & 1 & -\mu\end{bmatrix}, \tag{5.2}$$

$$\dot{\mathbf{v}}-A_2\mathbf{v}=\boldsymbol{\beta}\,e^{i\lambda t}+\boldsymbol{\gamma}\,e^{i\omega t}+(\text{c.c})+(\text{decay}), \tag{5.3}$$

(5.4)
$$\mathbf{v}=\alpha\, e^{i\lambda t}\left(0, 0, \frac{\mu+i\lambda}{1+i\lambda}, \mu+i\lambda, 1\right)^T + e^{i\lambda t}\left(\frac{\beta_1}{1+i\lambda}, \frac{\beta_2}{\mu+i\lambda}, \frac{\beta_3-\beta_5}{1+i\lambda}, -\beta_5, 0\right)^T$$
$$+e^{i\omega t}\left(\frac{\gamma_1}{1+i\omega}, \frac{\gamma_2}{\mu+i\omega}, \frac{\gamma_3+\Gamma}{1+i\omega}, \Gamma, \frac{\gamma_5+\Gamma}{\mu+i\omega}\right)^T + (\text{c.c}) + (\text{decay}),$$

(5.5)
$$(\sigma+\mu)(1-i\lambda)\beta_3+(1-\mu)\beta_4-(\sigma+1)(\mu-i\lambda)\beta_5=0,$$

in which $\boldsymbol{\beta}$ and $\boldsymbol{\gamma}$ are complex 5-dimensional column vectors, (c.c.) denotes complex conjugate, (decay) denotes decay terms, the real quantities λ and ω satisfy

(5.6)
$$\lambda=\left(\frac{\nu(1-\mu)}{\sigma+\mu}\right)^{1/2}, \qquad \omega\neq\lambda,$$

α is an arbitrary complex constant, and Γ is given by

(5.7)
$$\Gamma=[(1-\mu)(\Delta+i\omega)(\lambda^2-\omega^2)]^{-1}$$
$$\cdot[(\sigma+\mu)(1+\lambda^2)(\mu+i\omega)\gamma_3+(1-\mu)(1+i\omega)(\mu+i\omega)\gamma_4-(\sigma+1)$$
$$\cdot(\mu^2+\lambda^2)(1+i\omega)\gamma_5].$$

We deviate from the procedure in § 5 by relating the small parameters η and ε through the equation

(5.8)
$$\eta=k\varepsilon.$$

The quantity k is carried along as a parameter and, in the end, is recombined with ε and replaced by η. We emphasize that (5.8) is used for convenience only and is not at all necessary. The equations corresponding to (4.9) and (4.10) are

(5.9)
$$\mathbf{u}\sim\alpha(t)\, e^{i\lambda t}\left(0, 0, \frac{\mu+i\lambda}{1+i\lambda}, \mu+i\lambda, 1\right)^T+(\text{c.c.})+(\text{decay})+\sum_{j=1}^{\infty}\varepsilon^j\mathbf{u}^{(j)}(t; \alpha, \bar{\alpha}),$$

(5.10)
$$\dot{\alpha}(t)=\sum_{j=1}^{\infty}\varepsilon^j\alpha^{(j)}.$$

The first two terms on the right side of (5.9) are the solutions of the homogeneous system $\dot{\mathbf{u}}-A_2\mathbf{u}=0$ that correspond to the imaginary eigenvalues $\pm i\lambda$, while the (decay) terms in (5.9) correspond to the remaining eigenvalues of A_2 with negative real parts.

Proceeding in a manner analogous to § 4, we list the results in Appendix B. If we define the real functions $R(t)$ and $\psi(t)$ by

(5.11)
$$\varepsilon\alpha(t)=R(t)\varepsilon^{i\omega(t)},$$

then from (5.1), (5.9), and (B.1) we have for the solution $\mathbf{x}(t)$,

$$\begin{aligned}\mathbf{x}(t) \sim & R(t)\, e^{i(\lambda t+\psi(t))}(0, 0, (\mu+i\lambda)(1+i\lambda)^{-1}, \mu+i\lambda, 1)^T \\ & +\left(\delta-\left(\frac{\sigma+1}{\sigma+\mu}\right)\nu\right)[2\lambda(\lambda-i\Delta)(1+i\lambda)]^{-1}R(t)\, e^{i(\lambda t+\psi(t))} \\ & \cdot(0, 0, 1-\mu, (1+i\lambda^2), 0)^T \\ & -(\mu+i\lambda)R^2(t)\, e^{2i(\lambda t+\psi(t))}((\mu+i\lambda) \\ & \cdot(1+i\lambda)^{-1}(1+2i\lambda)^{-1}, (\mu+2i\lambda)^{-1}, 0, 0, 0)^T \\ & +(\text{c.c})+(\text{decay})-2R^2(t)((\mu^2+\lambda^2)(1+\lambda^2)^{-1}, 1, 0, 0, 0)+\cdots.\end{aligned} \tag{5.12}$$

From (5.8), (5.10), (B.2), (B.3), and (5.11), R satisfies

$$\begin{aligned}\frac{dR}{dt}=\frac{(1-\Delta)(\delta-((\sigma+1)/(\sigma+\mu)\nu)}{2(\lambda^2+\Delta^2)}R+\frac{3(\mu^2+\lambda^2)f(\lambda)}{2(\Delta^2+\lambda^2)(1+4\lambda^2)(\mu^2+4\lambda^2)}R^3+\cdots, \\ \delta-\left(\frac{\sigma+1}{\sigma+\mu}\right)\nu \ll 1,\end{aligned} \tag{5.13}$$

where $R(0)=O(\varepsilon)$ and

$$\begin{aligned}f(\lambda)=4\sigma\lambda^4-[7\mu\Delta+2\sigma\Delta+2\sigma\mu(\sigma+\mu)]\lambda^2 \\ -\mu\Delta[\Delta+\mu(\sigma+\mu)].\end{aligned} \tag{5.14}$$

Note that to the order of terms calculated, the oscillation at frequency λ appears only in the last three components of $\mathbf{x}$ in (5.12), while the frequency 2λ oscillation is present only in the first two components of $\mathbf{x}$. The phase $\psi(t)$ obeys an equation similar to (5.13) with the right hand side depending only on R. It is not reproduced here since its effect is just to introduce a slow variation in the phase of the oscillations. We note that (5.12), and thus also (5.13), cannot be valid when $\lambda=0$, which from (5.6) corresponds to $\nu=0$.

From (5.13), the behavior of $f(\lambda)$ (in particular its sign) is crucial in determining the evolution of the small-norm periodic oscillation, at frequency λ, near $L^{(2)}$. From (5.6) f is quadratic in ν, and it can be shown that f has only one real positive zero in ν at the value

$$\begin{aligned}\nu^{(3)}=&\frac{\sigma+\mu}{8\sigma(1-\mu)} \\ &\cdot[7\mu\Delta+2\sigma(\Delta+\mu(\sigma+\mu)) \\ &+[7\mu\Delta+2\sigma(\Delta+\mu(\sigma+\mu))]^2+16\mu\sigma\Delta(\Delta+\mu(\sigma+\mu))]^{1/2}].\end{aligned} \tag{5.15}$$

This is just the abscissa of the point labeled $P^{(3)}$ in Fig. 1. It is also easily shown that

$$\nu^{(3)}>\nu^{(2)}, \tag{5.16}$$

and thus $P^{(3)}$ lies to the right of $P^{(2)}$ in Fig. 1.

We can now ascertain the following behavior of solutions of (5.13):

$\nu<\nu^{(3)}$:

(a) Close to and above the line $L^{(2)}$, i.e., $\delta>((\sigma+1)/(\sigma+\mu))\nu$, the coefficients of the R and R^3 terms in (5.13) are negative. Thus an initially small disturbance approaches zero as $t \to \infty$, exponentially but with superposed oscillations.

(b) Near and below $L^{(2)}$, where $\delta < ((\sigma+1)/(\sigma+\mu))\nu$, a small-norm disturbance grows, in an oscillatory manner. To leading order, the components x_3, x_4, and x_5 of $\mathbf{x}$ of (5.12) attain an oscillation with frequency λ given by (5.6). The amplitude of the oscillation is small, of order $(|\delta - ((\sigma+1)/(\sigma+\mu))\nu|)^{1/2}$, and is given by the nonzero value of R which causes the right side of (5.13) to vanish. These results for $\nu < \nu^{(3)}$ are typical of so-called Hopf bifurcation [8].

$\nu > \nu^{(3)}$:

(a) Close to and above $L^{(2)}$ where $\delta > ((\sigma+1)/(\sigma+\mu))\nu$, the coefficient of the R term in (5.13) is negative but the coefficient of the R^3 term is positive. In this case, typical of subcritical instability, initially very small perturbations decay to zero, while somewhat larger ones grow out of the small-norm regime. The size of initial perturbations which demarcates this behavior is evidently not easily specified, since $\mathbf{x}$ is a five-component vector.

(b) Near and below $L^{(2)}$, (5.13) predicts that the solution $\mathbf{x}$ in (5.12) will grow out of the small-norm regime.

The occurrence of the point $P^{(3)}$ on $L^{(2)}$ is particularly striking. The line $L^{(2)}$, where some eigenvalues of the linearized system become purely imaginary, is a prime location for possible bifurcation of periodic solutions. The above results indicate that, for $\nu < \nu^{(3)}$, we will have "supercritical" Hopf bifurcation, in which solutions near and to the right of $L^{(2)}$ will proceed to a stable, small-norm periodic solution. However, for $\nu > \nu^{(3)}$, we have "subcritical" Hopf bifurcation, for which all solutions grow out of the small-norm regime. This behavior is, of course, a nonlinear time-dependent phenomenon and could not have been ascertained from the discussions in §§ 2 and 3. Numerical calculations of the complete system (2.2) indicate that small-norm disturbances evolve differently for large time depending on whether ν is less or greater than $\nu^{(3)}$. Further investigations are in progress and will be reported elsewhere.

The point $P^{(3)}$ is also interesting in view of calculations by Sani [9] for double-diffusive convection with the Navier–Stokes equations. Bifurcation in the Navier–Stokes problem has a structure remarkably similar to that in our fluid-loop model. There are direct analogues of our linear stability boundaries $L^{(1)}$ and $L^{(2)}$, and our parabolic global stability boundary is exactly the same as found by Joseph [3]. Moreover, Sani's calculations using the Stuart–Watson method produced a point analogous to $P^{(1)}$, where the coefficient of the cubic term in the amplitude equation for steady bifurcation vanishes. However, Sani did not discover the existence of a point analogous to $P^{(3)}$, finding instead a result corresponding to $f(\lambda) \equiv 0$. A reinvestigation of the problem with the Navier–Stokes equations will also be reported later.

6. Dynamic behavior near $P^{(0)}$. Setting $\delta = \nu = 0$ in (2.3), we can easily show that the linear matrix A has a double zero eigenvalue, with only one eigenvector. We cannot proceed as in §§ 4 and 5 since the leading-order term in a formal asymptotic expansion would necessarily have a linear growth term in t. To overcome this difficulty, we first make a change of variables and then scale the new variables appropriately so that the new leading-order linear matrix has a double zero eigenvalue and two linearly independent eigenvectors corresponding to it. This is equivalent to what was done in [15].

We define the quantities v_i, $1 \leqq i \leqq 5$, by

$$v_1 = \varepsilon^{-1} x_1, \quad v_2 = \varepsilon^{-1} x_2, \quad v_3 = \varepsilon^{-1} x_3, \tag{6.1}$$
$$v_4 = \varepsilon^{-3/2}(-x_3 + x_4), \qquad v_5 = \varepsilon^{-2}\left(\frac{\sigma+1}{1-\mu}\right)[x_3 - (1-\mu)x_4 - \mu^2 x_5].$$

We also define k_1 and k_2 by

$$\delta = k_1 \varepsilon, \qquad \nu = k_2 \varepsilon, \tag{6.2}$$

which is analogous to what was done in § 5. The quantities k_1 and k_2 will be treated as parameters in the calculations and replaced ultimately by δ and ν. Then, in terms of the parameter

$$\theta = \varepsilon^{1/2}, \tag{6.3}$$

equations (2.2) and (2.3) become

$$\begin{aligned}
\dot{\mathbf{v}} &= A_0 \mathbf{v} + \left(0, 0, 0, 0, \left(\frac{1+\sigma}{1-\mu}\right) v_3(v_1 - \mu^2 v_2)\right)^T \\
&\quad + \theta\left[B_0 \mathbf{v} + \left(0, 0, 0, -v_1 v_3, \left(\frac{1+\sigma}{1-\mu}\right) v_4(v_1 - \mu^2 v_2)\right)^T\right] \\
&\quad + \theta^2[C_0 \mathbf{v} + (-v_3^2, -\mu^{-1} v_3^2, v_1 v_3, -v_1 v_4, 0)^T] \\
&\quad + \theta^3\left(-v_3 v_4, (1-2\mu)\mu^{-2} v_3 v_4, v_1 v_4, \frac{k_1(1-\mu)\mu^{-2} v_5}{(1+\sigma)}, 0\right)^T \\
&\quad + \theta^4\left(0, (1-\mu)\mu^{-2} v_4^2 + \frac{(1-\mu)\mu^{-2}}{(1+\sigma)} v_3 v_5, 0, 0, 0\right)^T \\
&\quad + \theta^5\left(0, \frac{(1-\mu)\mu^{-2}}{(1+\sigma)} v_4 v_5, 0, 0, 0\right)^T,
\end{aligned} \tag{6.4}$$

where

$$A_0 = \begin{bmatrix} -1 & 0 & 0 & 0 & 0 \\ 0 & -\mu & 0 & 0 & 0 \\ 0 & 0 & 0 & 0 & 0 \\ 0 & 0 & 0 & 0 & 0 \\ 0 & 0 & \kappa & 0 & -\Delta \end{bmatrix}, \quad B_0 = \begin{bmatrix} 0 & 0 & 0 & 0 & 0 \\ 0 & 0 & 0 & 0 & 0 \\ 0 & 0 & 0 & 1 & 0 \\ 0 & 0 & \dfrac{-\kappa}{(1+\sigma)} & 0 & 1 \\ 0 & 0 & 0 & \dfrac{-k_1(1-\mu)(1+\sigma)}{\mu^2} & 0 \end{bmatrix},$$

(6.5)

$$C_0 = \begin{bmatrix} 0 & 0 & 0 & 0 & 0 \\ 0 & 0 & 0 & 0 & 0 \\ 0 & 0 & 0 & 0 & 0 \\ 0 & 0 & 0 & \dfrac{k_1(1-\mu)}{\mu^2} & 0 \\ 0 & 0 & 0 & 0 & \dfrac{-k_1(1-\mu)}{\mu^2} \end{bmatrix}, \quad \kappa = \mu^{-1}(1+\sigma)(k_1 - \mu k_2).$$

To solve (6.4) we assume that the solution has the form

$$\mathbf{v} \sim \alpha_1 e^{-t}\left(1, 0, 0, 0, \frac{\Delta(1+\sigma)\alpha_3}{(1-\mu)(\sigma+\mu)}\right)^T + \alpha_2 e^{-\mu t}\left(0, 1, 0, 0, \frac{-\mu^2\Delta\alpha_3}{1-\mu}\right)^T$$

$$(6.6) \qquad + \alpha_3(0, 0, \Delta, 0, \kappa)^T + \alpha_4(0, 0, 0, 1, 0)^T$$

$$+ \theta^{-2}\alpha_5 e^{-\Delta t}(0, 0, 0, 0, 1)^T + \sum_{j=-1}^{\infty} \theta^j \mathbf{v}^{(j)}(t, \boldsymbol{\alpha}),$$

where

$$(6.7) \qquad \dot{\alpha}_j \doteq \sum_{k=1}^{\infty} \alpha_j^{(k)}\theta^k, \qquad 1 \leqq j \leqq 5.$$

The first five terms on the right side of (6.6) constitute the most general solution of the leading order nonlinear system derived from (6.4) upon setting $\theta = 0$. The terms involving α_3 and α_4 are multiples of the two linearly independent eigenvectors of A_0 corresponding to the double zero eigenvalue. Note that the term in (6.6) involving $\alpha_5 e^{-\Delta t}$ is multiplied by θ^{-2} as a consequence of the scaling used in (6.1). The difficulty the scaling (6.1) overcomes is the occurrence of a double zero eigenvalue, with a single eigenvector, of the original matrix. However, because of the structure of this matrix, in particular the way the eigenvalue $-\Delta$ enters, the leading-order solution $\mathbf{x}$ of (2.2) will in general contain $e^{-\Delta t}$ terms. The scaling (6.1) estimates the fifth component of $\mathbf{x}$, and thus the $e^{-\Delta t}$ terms, as small of order θ^2. Therefore, this scaling must be revised by a θ^{-2} factor in the $e^{-\Delta t}$ term of v_5, and the $\theta^{-1}\mathbf{v}^{(-1)}$ term in (6.6) is of course needed in order to accommodate the θ^{-2} term.

Our calculational procedure here differs somewhat from those in §§ 4 and 5, because we must now perturb from a nonlinear system instead of a linear system. For this reason, we show the calculation of the θ^{-1} terms in (6.6). The equations governing them are:

$$(6.8) \qquad v_{1t}^{(-1)} + v_1^{(-1)} = 0,$$

$$(6.9) \qquad v_{2t}^{(-1)} + \mu v_2^{(-1)} = 0,$$

$$(6.10) \qquad v_{3t}^{(-1)} = 0,$$

$$v_{4t}^{(-1)} = \alpha_5 e^{-\Delta t} - v_1^{(-1)} v_3^{(-1)}, \tag{6.11}$$

$$\begin{aligned} v_{5t}^{(-1)} + \Delta v_5^{(-1)} = & -\alpha_5^{(1)} e^{-\Delta t} + \kappa v_3^{(-1)} \\ & + \left(\frac{1+\sigma}{1-\mu}\right)[v_3^{(-1)}(\alpha_1 e^{-t} - \mu^2 \alpha_2 e^{-\mu t} + v_1^{(0)} - \mu^2 v_2^{(0)}) \\ & + (v_1^{(-1)} - \mu^2 v_2^{(-1)})(\Delta\alpha_3 + v_3^{(0)}) + v_4^{(-1)}(v_1^{(-1)} - \mu^2 v_2^{(-1)})]. \end{aligned} \tag{6.12}$$

Solving (6.8)–(6.11) we get

$$\begin{aligned} & v_1^{(-1)} = \beta_1 e^{-t}, \quad v_2^{(-1)} = \beta_2 e^{-\mu t}, \quad v_3^{(-1)} = \beta_3, \\ & v_4^{(-1)} = \beta_4 - \Delta^{-1}\alpha_5 e^{-\Delta t} + \beta_1\beta_3 e^{-t}, \end{aligned} \tag{6.13}$$

where β_i $(1 \leqq i \leqq 4)$ are constants of integration. The appearance of $v_{1,2,3}^{(0)}$ on the right side of (6.12) indicates that the asymptotic sequence of equations is not a closed system. However, using the results (6.13), we can eliminate the $\mathbf{v}^{(0)}$ terms from the right side of (6.12) (and close the system) by choosing

$$\beta_1 = \beta_2 = \beta_3 = 0, \tag{6.14}$$

which yields

$$v_1^{(-1)} = v_2^{(-1)} = v_3^{(-1)} = 0. \tag{6.15}$$

We note that results analogous to (6.14) arose in §§ 4 and 5 by eliminating the homogeneous solutions of the basic linear system.

With (6.14) we can solve (6.12) and obtain the bounded vector

$$\begin{aligned} \mathbf{v}^{(-1)} = & \beta_4(0, 0, 0, 1, 0)^T + \beta_5 e^{-\Delta t}(0, 0, 0, 0, 1)^T \\ & + e^{-\Delta t}(0, 0, 0, -\Delta^{-1}\alpha_5, 0)^T, \end{aligned} \tag{6.16}$$

$$\alpha_5^{(1)} = 0, \tag{6.17}$$

where condition (6.17) follows from requiring boundedness of $v_5^{(-1)}$. Since the first two terms on the right side of (6.16) are precisely of the form of the fourth and fifth terms on the right side of (6.6), these terms should be eliminated in order to continue the analogy with requirements in previous sections, i.e.,

$$\beta_4 = \beta_5 = 0. \tag{6.18}$$

We remark that the $\mathbf{v}^{(0)}$ term as well as the $\mathbf{v}^{(-1)}$ term on the right side of (6.6) can be shown to consist of decaying terms, and that the $O(\theta^{-1})$ and $O(\theta^{-2})$ terms in (6.6) are no bigger than $O(\varepsilon)$ in $\mathbf{x}$ (see (6.1)). Thus, the terms of principal concern in (6.6) for the dynamical behavior near $P^{(0)}$ are those involving α_3 and α_4.

Proceeding as above, we find without further complications that the equations governing the time behavior of α_3 and α_4 decouple from those governing α_1, α_2, and α_5. Eliminating α_4 to obtain a single second-order equation for α_3, defining an amplitude function R by

$$R \equiv \Delta\alpha_3\theta^2, \tag{6.19}$$

and using (6.2) and (6.3), we see that R satisfies the nonlinear equation

$$\begin{aligned}\ddot{R}+\frac{(\sigma+\mu)}{\Delta^2}\left(\delta-\left(\frac{\sigma+1}{\sigma+\mu}\right)\nu\right)\dot{R}\\ +\frac{(\delta-\mu\nu)}{\Delta}\left[1+\Delta^{-3}(\sigma+\mu)\left(\delta-\left(\frac{\sigma+1}{\sigma+\mu}\right)\nu\right)\right]R-R^3=0,\end{aligned} \tag{6.20}$$

and the solution vector $\mathbf{x}$, to the order completed, satisfies

$$\mathbf{x}(t)=(0,0,R,R+\dot{R},\mu^{-2}(\mu R-(1-\mu)\dot{R}))^T+(\text{decay}). \tag{6.21}$$

We omit the calculation of initial conditions on R, from (2.2), (6.1), and (6.6), since the qualitative features of solutions of (6.20) can be discussed without explicit initial conditions. Note that the linear growth rates, obtained by ignoring the R^3 term in (6.20), are determined by the quadratic

$$\begin{aligned}\lambda_0^2+\frac{(\sigma+\mu)}{\Delta^2}\left(\delta-\left(\frac{\sigma+1}{\sigma+\mu}\right)\nu\right)\lambda_0\\ +\frac{(\delta-\mu\nu)}{\Delta}\left[1+\Delta^{-3}(\sigma+\mu)\left(\delta-\left(\frac{\sigma+1}{\sigma+\mu}\right)\nu\right)\right]=0,\end{aligned} \tag{6.22}$$

which is exactly the first few terms of the linear growth rate equation given in (2.10) and (2.11). Also, if the scaling (6.1) were not made, then a restriction on the initial conditions similar to that discussed in [15] and [16] would be necessary to eliminate a linear time growth term.

A simple phase plane analysis of (6.20) reveals the following characteristics of the time behavior of the amplitude $R(t)$:

(a) On and below the solid portion of line $L^{(1)}$, and below the solid portion of line $L^{(2)}$, almost every solution of (6.20) is unbounded. The only exceptional solutions are those represented by separatrices in the phase plane, i.e., a few trajectories in the phase plane which enter unstable singular points (corresponding to the zero solution and, above the dashed portion of $L^{(1)}$, the unstable small-norm steady solutions). The fact that solutions of (6.20) become unbounded only means that there are no small-norm solutions of our original system.

(b) On the solid portion of line $L^{(2)}$, stable periodic solutions of small norm exist. This is not unexpected, since on $L^{(2)}$ the linear matrix A has conjugate purely imaginary eigenvalues. However, there are also unbounded solutions here. Thus, the zero solution is stable (but not asymptotically stable) to small enough perturbations and unstable to sufficiently large perturbations.

(c) Above the solid portions of both $L^{(1)}$ and $L^{(2)}$, the zero solution in the phase plane is a stable spiral or nodal point. This is due to the fact that this region is inside the linear stability boundary. Sufficiently large perturbations will become unbounded, however.

In the context of these results, it is very interesting to recall that near the solid portion of $L^{(2)}$, but away from $P^{(0)}$, bifurcation of the Hopf type occurs. That is, away from $P^{(0)}$ and below $L^{(2)}$, a small-norm periodic solution exists. The situation is quite different near $P^{(0)}$. Evidently, as $P^{(0)}$ is approached the stable small-norm periodic solution, which exists below $L^{(2)}$, is affected by the existence of the double zero eigenvalue at $P^{(0)}$ and evolves out of the small norm regime.

It is also worth mentioning that below both solid and dashed portions of $L^{(1)}$, the phase plane analysis shows that solutions of (6.20) become unbounded without oscillations. Thus, below $L^{(1)}$, the oscillatory nature of the bifurcation is completely absent. Above $L^{(1)}$, on the other hand, there are at least vestigial elements of the oscillatory character of Hopf bifurcation, even though strictly periodic solutions of small norm exist only on the solid portion of $L^{(2)}$. Moreover, on this solid portion of $L^{(2)}$, there are infinitely many small-norm periodic solutions, unlike the situation below $L^{(2)}$ away from $P^{(0)}$, where an oscillation of given amplitude exists (see (5.13)). Finally, note that near the solid portion of $L^{(1)}$, (6.20) is in some sense the limiting version of (4.19). This connection cannot be rigorously valid, since (4.19) obviously fails as ν approaches zero. However, if in (6.20) the $\ddot{R}$ term is deleted and δ is assumed close to $\mu\nu$, then the terms in the resulting equation correspond naturally to terms in (4.19).

It is anticipated that analogous results to those in this section apply near the point corresponding to $P^{(0)}$ in the appropriate parameter plane for double diffusion with the Navier–Stokes equations. Calculations for the amplitude equation near this point were made by Sani [9] using the Stuart–Watson technique. Sani did not construct a second-order equation analogous to (6.20). Instead, he found a first-order equation with certain coefficients that became singular approaching the analogue of $P^{(0)}$. We believe the occurrence of a double zero eigenvalue necessitates an amplitude equation of the type (6.20) for the problem with the Navier–Stokes equations, and the derivation of it using procedures similar to those presented here will be reported elsewhere.

Appendix A. The functions appearing in (4.20) are given by

$$\begin{aligned}\mathbf{x}_1^{(0)} = {} & -R^2(t)(\mu^2, 1, 0, 0, 0)^T - \mu^2\nu^{-1}(1-\mu)^{-1} \\ & \cdot R^3(t)(0, 0, \Delta(1-\mu), \nu(1-\mu)+\Delta, 0)^T \\ & + \nu^{-1}(1-\mu)^{-1}R^4(t)(\Delta\mu^3(2-3\mu) - \mu^3\nu(1-\mu)(1+2\mu), \\ & \qquad -\mu\Delta - \nu(1-\mu)(2+\mu), 0, 0, 0)^T,\end{aligned} \tag{A.1}$$

$$\begin{aligned}\mathbf{x}_1^{(1)} = {} & \nu^{-1}(1-\mu)^{-1}R(t)(0, 0, 1-\mu, 1, 0)^T \\ & + \nu^{-1}(1-\mu)R^2(t)(\mu(3\mu-2), \mu^{-1}, 0, 0, 0)^T \\ & - \mu\nu^{-3}(1-\mu)^{-3}R^3(t)(0, 0, K_2, K_1, 0)^T,\end{aligned} \tag{A.2}$$

$$\begin{aligned}\mathbf{x}_1^{(2)} = {} & \nu^{-3}(1-\mu)^{-3}R(t)(0, 0, (1-\mu)\Delta, \nu(1-\mu)+\Delta, 0)^T \\ & - R^2(t)\nu^{-3}(1-\mu)^{-3}(K_3, K_4, 0, 0, 0)^T,\end{aligned} \tag{A.3}$$

$$\begin{aligned}\mathbf{x}_1^{(3)} = {} & \nu^{-5}(1-\mu)^{-5}R(t)(0, 0, (1-\mu)(2\Delta^2 + \nu(1-\mu)(1+\Delta)), \\ & \qquad (\nu(1-\mu)+\Delta)^2 + \nu(1-\mu)(1+\Delta) + \Delta^2, 0)^T,\end{aligned} \tag{A.4}$$

where

$$K_1 = \nu^2(1-\mu)^2(1-2\mu) + \nu(1-\mu)(6\mu + \Delta(1+2\mu)) + 4\mu\Delta^2, \tag{A.5}$$

$$K_2 = (1-\mu)[\nu(1-\mu)(6\mu + \Delta - 2\mu\Delta) + 4\mu\Delta^2], \tag{A.6}$$

$$K_3 = \nu(1-\mu)(1-2\mu)^2 + \mu\Delta(2-3\mu), \tag{A.7}$$

(A.8) $K_4 = \mu^{-2}[\nu(1-\mu)(2-\mu)-\mu\Delta]$.

The constants K_5, K_6 and K_7 in (4.21) are

(A.9) $K_5 = \nu^{-5}(1-\mu)^{-5}[(\nu(1-\mu)+\Delta)^2+\nu(1-\mu)(\Delta+1)+\Delta^2]$,

(A.10)
$$K_6 = \nu^{-7}(1-\mu)^{-7}[(\Delta+\nu(1-\mu))^3+(3\Delta+2)(\Delta+\nu(1-\mu))^2 + (\Delta^2-\Delta+2\nu(1-\mu))(\Delta+\nu(1-\mu))-\Delta^2],$$

(A.11) $K_7 = -\mu\nu^{-3}(1-\mu)^{-3}K_1$.

Appendix B. The functions $\mathbf{u}^{(j)}$ appearing in (5.9) and the constants $\alpha^{(j)}$ in (5.10) are given by

(B.1)
$$\begin{aligned}\mathbf{u}^{(1)} = {}&[2\lambda(\lambda-i\Delta)(1+i\lambda)]^{-1}k\alpha\, e^{i\lambda t}(0,0,1-\mu,(1+i\lambda)^2,0)^T\\ &-(\mu+i\lambda)\alpha^2 e^{2i\lambda t}((\mu+i\lambda)\\ &\qquad(1+i\lambda)^{-1}(1+2i\lambda)^{-1},(\mu+2i\lambda)^{-1},0,0,0)^T\\ &+(\text{c.c.})-2|\alpha|^2((\mu^2+\lambda^2)(1+\lambda^2)^{-1},1,0,0,0)^T,\end{aligned}$$

(B.2) $\alpha^{(1)} = k[2\lambda(\lambda-i\Delta)]^{-1}(1+i\lambda)\alpha$,

(B.3)
$$\begin{aligned}\alpha^{(2)} = {}&k^2(1+i\lambda)(\Delta-\lambda^2+i\lambda(2-\sigma-\mu))[8\lambda^3(\lambda-i\Delta)^3]^{-1}\alpha\\ &-3i(\mu^2+\lambda^2)(\mu+i\lambda)(\Delta+2i\lambda)(1+i\lambda)\\ &\cdot[2\lambda(\Delta+i\lambda)(1+2i\lambda)(\mu+2i\lambda)]^{-1}\alpha|\alpha|^2.\end{aligned}$$

The vector $\mathbf{u}^{(2)}$ has been computed and is quite lengthy.

REFERENCES

[1] J. S. TURNER, *Buoyancy Effects in Fluids*, Cambridge University Press, London, 1973.

[2] W. L. SIEGMANN AND L. A. RUBENFELD, *A nonlinear model for double-diffusive convection*, this Journal, 29 (1975), pp. 540–557.

[3] D. D. JOSEPH, *Global Stability of Fluid Motions*, Tracts in Natural Philosophy, Springer-Verlag, Berlin, 1976.

[4] D. SATTINGER, *Topics in Stability and Bifurcation Theory*, Lecture Notes in Mathematics, Springer-Verlag, Berlin, 1973.

[5] I. STAKGOLD, *Branching of solutions of nonlinear equations*, SIAM Rev., 13 (1971), pp. 289–332.

[6] G. H. PIMBLEY, JR., *Eigenfunction Branches of Nonlinear Operators and their Birfurcations*, Lecture Notes in Mathematics, Springer-Verlag, Berlin, 1969.

[7] V. M. VOLOSOV, *Averaging in systems of ordinary differential equations*, Russian Math. Surveys, 7 (1972), no. 17, pp. 1–126.

[8] E. HOPF, *Bifurcation of a periodic solution from a stationary solution of a system of differential equations*, Berichten der Sächsischen Akad. der Wissenschaften, Liepzig (1942).

[9] R. L. SANI, *On finite amplitude roll cell disturbances in a fluid layer subjected to heat and mass transfer*, A.I.Ch.E.J., 11 (1965), pp. 971–980.

[10] I. STAKGOLD, D. JOSEPH AND D. SATTINGER, *Nonlinear Problems in the Physical Sciences and Biology*, Lecture Notes in Mathematics, no. 332, Springer-Verlag, Berlin, 1973.

[11] B. MATKOWSKY, *A simple nonlinear dynamic stability problem*, Bull. Amer. Math. Soc., 17 (1970), pp. 620–625.

[12] S. KOGELMAN AND J. B. KELLER, *Transient behavior of unstable nonlinear systems with applications to the Bernard and Taylor problems*, this Journal, 20 (1971), pp. 619–637.

[13] J. T. STUART, *On the non-linear mechanics of wave disturbances in stable and unstable parallel flows, Part 1*, J. Fluid Mech., 9 (1970), pp. 353–370.

[14] J. WATSON, *On the non-linear mechanics of wave disturbances in stable and unstable parallel flows, Part 2*, Ibid., 9 (1970), pp. 371–389.

[15] L. A. RUBENFELD, *Nonlinear dynamic buckling of a compressed elastic column*, Quart. Appl. Math., 32 (1974), pp. 163–171.

[16] E. REISS AND B. MATKOWSKY, *Nonlinear dynamic buckling of a compressed elastic column*, Ibid., 29 (1971), pp. 245–260.

[17] L. A. RUBENFELD, *On a derivative-expansion technique and some comments on multiple scaling in the asymptotic approximation of solutions of certain differential equations*, SIAM Rev., to appear.

[18] R. A. STRUBLE, *Nonlinear Differential Equations*, McGraw-Hill, New York, 1962.